View metadata, citation and similar papers at core.ac.uk
brought to you by CORE
provided by Elsevier - Publisher Connector

Kidney International, Vol. 64 (2003), pp. 1722–1732

Selective depletion of fibroblasts preserves morphology and the functional integrity of peritoneum in transgenic mice with peritoneal fibrosing syndrome[1]

Hirokazu Okada, Tsutomu Inoue, Yoshihiko Kanno, Tatsuya Kobayashi, Yusuke Watanabe, Shinichi Ban, Eric G. Neilson, and Hiromichi Suzuki

Department of Nephrology and Department of Pathology, Saitama Medical College, Saitama, Japan; and Division of Nephrology and Hypertension, Department of Medicine and Department of Cell and Developmental Biology, Vanderbilt University School of Medicine, Nashville, Tennessee

Selective depletion of fibroblasts preserves morphology and the functional integrity of peritoneum in transgenic mice with peritoneal fibrosing syndrome.

Background. A peritoneal fibrosing syndrome (PFS) can progressively reduce peritoneal ultrafiltration during chronic peritoneal dialysis in patients with renal failure. The pathogenesis of PFS is unclear and the role of peritoneal fibroblasts has not been evaluated experimentally.

Methods. We followed the fate of fibroblasts producing PFS in a mouse model using fibroblast-specific protein 1 (FSP1) as a marker. PFS was induced by daily peritoneal infusions of chlorhexidine gluconate (CHG) saline into transgenic mice expressing the thymidine kinase (Δtk) gene under the control of the *FSP1* promoter (FSP1.Δtk mice). To demonstrate the role of fibroblasts in PFS, we treated these FSP1.Δtk mice with a nucleoside analogue to induce DNA chain termination and fibroblast death.

Results. Mice receiving peritoneal infusions of CHG saline every other day for 2 weeks developed increasing numbers of $FSP1^+$ fibroblasts in the subserosal layers of the visceral peritoneum. Mac-3^+ monocytes (macrophages) subsequently accumulated over the next 2 weeks in association with increased deposition of type I collagen and increased endothelial vascularity ($CD31^+$) in these subserosal tissues. Since these peritoneal fibroblasts expressed monocyte chemoattractant protein-1 (MCP-1), heat shock protein 47 (HSP47), and vascular endothelial growth factor (VEGF), we suspect they were partially responsible for macrophage recruitment, matrix production, and the neoangiogenesis in the subserosal tissue. Treatment of PFS in FSP1.Δtk transgenic mice with a nucleoside analogue selectively reduced the numbers of peritoneal fibroblasts and attenuated the attendant changes in peritoneal histology. Rescuing the peritoneal membrane from chronic thickening and neoangiogenesis by reducing the number of fibroblasts also preserved ultrafiltration.

Conclusion. Peritoneal fibroblasts play a pivotal role in PFS, and their deletion using a fibroblasts-specific transgene was effective in preventing peritoneal fibrogenesis.

There is a tendency to lose peritoneal ultrafiltration and small molecule clearance [1–5] in patients receiving continuous ambulatory peritoneal dialysis (CAPD). Within a few months to a year after the initiation of CAPD, peritoneal membranes undergo a structural deterioration [2, 5–12] associated with membrane thickening and fibrosis [13]. This disorder is called the peritoneal fibrosing syndrome (PFS) [14]. Preserving the longevity of the peritoneal membrane and its relationship to normal peritoneal physiology is important to the long-term success of this therapy [1, 2, 5].

The expression of PFS is variable in humans, depending on individual susceptibility to membrane damage or the type of dialysate used for therapy. Long-term use of nonphysiologic dialysis fluids (low pH, hyperosmolarity, high glucose concentration, or high lactate), or contaminants derived from the nonenzymatic degradation of glucose, repeated bacterial peritonitis, or exposure to some drugs and antiseptics all contribute to PFS [2, 5, 14, 15]. The expected pathology in PFS seems independent of its cause [10, 12, 14, 16]. There have been several animal models of PFS, some of which are generated by substances currently unused for CAPD patients such as chlorhexidine [17–25]. However, these models share a number of similarities to human PFS [13] and have contributed to its understanding. The role of fibroblasts in the alteration of the peritoneum has never been studied in detail because of a dearth of fibroblast-specific markers.

Several years ago, we cloned fibroblast-specific protein 1

[1]**Jared Grantham, M.D., served as guest editor for this paper.**

Key words: FSP1, monocytes/macrophages, type I collagen, monocyte chemoattractant protein-1, heat shock protein 47, vascular endothelial growth factor.

Received for publication July 5, 2002
and in revised form April 15, 2003
Accepted for publication July 8, 2003

© 2003 by the International Society of Nephrology

(FSP1) [26, 27] and demonstrated the presence of fibroblasts in fibrosing tissues using anti-FSP1 antibodies [27–29]. $FSP1^+$ fibroblasts remodel tissue architecture in organ fibrosis [27, 29]. When inflammation initiates tissue fibrogenesis, $FSP1^+$ fibroblasts activate, proliferate, and produce fibrogenic molecules such as type I and III collagens, fibronectin, and proteoglycans [27, 29]. When tissue inflammation resolves, $FSP1^+$ fibroblasts attenuate through apoptosis, leaving an acellular fibrous scar. With FSP1 as a marker, we studied a murine model of PFS to monitor the cell fate and pathophysiologic role of fibroblasts in the peritoneum challenged by chlorhexidine [30]. Transgenic mice (FSP1.Δtk) whose fibroblasts selectively express high levels of herpes simplex virus thymidine kinase (Δtk) under the control of the FSP1 promoter [26, 31] were treated with gancyclovir (GCV), a nucleoside analogue, which corrupts DNA synthesis by chain termination in dividing cells [31]. By generating PFS in FSP1.Δtk mice we asked if fibroblasts depletion would attenuate peritoneal histopathology or its functional deterioration.

We also focused on the role of macrophages in this study as they are a source of profibrotic molecules, including transforming growth factor-β1 (TGF-β1), platelet-derived growth factor (PDGF), tumor necrosis factor-α (TNF-α), interleukin-1 (IL-1), and fibronectin [29, 32]. These macrophages migrate to the peritoneal interstitium and peritoneal fluid from the circulation through small blood vessels [33]. The stimulus for this efflux is thought to be chemoattractant molecules, like monocyte chemoattractant protein-1 (MCP-1), regulated upon activation, normal T cell expressed and secreted (RANTES), macrophage inflammatory protein-1 (MIP-1), which are secreted by a variety of resident cells such as mesothelial cells, fibroblasts, or previously recruited macrophages [32, 34].

METHODS

Transgenic mice

FSP1.Δtk mice were housed individually with free access to chow and water and with humidity and temperature controlled under pathogen-free conditions. Animal care and treatment conformed to institutional guidelines. The creation of FSP1.Δtk mice and their breeding onto a Balb/c background has been previously described [31]. The FSP1 promoter directs the expression of Δtk exclusively in $FSP1^+$ fibroblasts making these fibroblasts selectively susceptible to the lethal effects of nucleoside analogues either in culture or during experimental fibrosis [26, 31].

Generation of PFS in FSP1.Δtk or wild-type mice

Six 8-week-old male mice were maintained chronically with 21 gauge plastic catheters (Terumo, Tokyo, Japan) inserted from a position along the high back, through the retroperitoneum, into the peritoneal cavity. Peritoneal fibrosis developed in peritoneal fibrosis mice following intraperitoneal injections of 0.03% chlorhexidine gluconate and 5% ethanol dissolved in 1.0 mL of saline (CHG saline) through a catheter every other day for 4 weeks. Control mice were treated with normal saline. Optimal conditions for producing chronic peritonitis with fibrogenesis were first determined in pilot studies (data not shown). In these early pilot studies, there were no substantial differences in pathology between the visceral and parietal peritoneum in peritoneal fibrosis mice with PFS at week 4. Since the surface area of visceral peritoneum is significantly larger and potentially more important as dialysis membrane, and since solid samples of bowel are easier to process, we used visceral peritoneum for our pathologic analyses. To minimize loss of mesothelium during tissue harvest, the rest of the intestines were immediately fixed in 4% paraformaldehyde [phosphate-buffered saline (PBS)] overnight, and then at least 10 small cylindric samples of bowel wall were randomly cut from fixed intestine and mounted in paraffin with the axis being kept vertical to the horizontal surface of the paraffin block. These tissue samples were used for histopathology and immunohistochemical analyses. The rest of the fixed bowel samples were rinsed in serial concentrations of sucrose solution and then snap-frozen for immunofluorescence.

Deletion of peritoneal fibroblasts in FSP1.Δtk or wild-type mice

To evaluate the effects of GCV on the deletion of fibroblasts in PFS, FSP1.Δtk (transgenic) or wild-type mice were divided into four comparative groups: peritoneal fibrosis-transgenic, control-transgenic, peritoneal fibrosis–wild-type, and control-wild-type mice. Peritoneal fibrosis-transgenic mice ($N = 10$) and peritoneal fibrosis-wild-type mice ($N = 10$) were treated with a catheter injection of 1.0 mL of CHG saline at 9:00 a.m. every other day for 4 weeks. Two weeks after initiation of CHG saline injections, GCV (kindly provided by F. Hoffmann, La Roche, Ltd., Basel, Switzerland) in PBS was also injected through the catheter (50mg/kg weight) at 9:00 p.m. every day for 2 weeks. Control-transgenic mice ($N = 8$) and control-wild-type mice ($N = 9$) received normal saline instead of CHG saline as above, and were likewise treated with GCV over the last 2 weeks of the experiment. During the study, mice losing a catheter were excluded from the data analysis (three mice from the control groups). Preliminary studies revealed that 2 weeks of GCV treatment did not yield any pathology in the peritoneal tissue of transgenic or wild-type mice (data not shown). All groups therefore received GCV in these experiments. At the end of the study, a modified peritoneal equilibrium test (PET) was carried out on each test subject and then tissue samples

were harvested for histopathologic evaluation and direct enzyme-linked immunosorbent assay (ELISA).

Flow cytometric analyses

Splenocytes were liberated from the spleens of peritoneal fibrosis-transgenic, peritoneal fibrosis-wild-type, control-transgenic, and control-wild-type mice by sieving through a nylon mesh. The cells were washed in PBS four times, and then incubated in hemolysis buffer (0.15 mol/L NH_4Cl, 1 mmol/L $KHCO_3$, 0.1 mmol/L Na_2 ethylenediaminetetraacetic acid (EDTA) at pH 7.4) at room temperature for 5 minutes with occasional shaking [35]. The splenocytes were next washed in staining buffer [PBS with 1% bovine serum albumin (BSA)] four times and 50 μL aliquots of 10^6 cells were then incubated with various antibodies: monoclonal rat antimouse macrophages (Mac-3) (1:50) (PharMingen, San Diego, CA, USA), or fluorescein isothiocyanate (FITC)-conjugated rat antimouse CD4 or antimouse CD8 (PharMingen) for 20 minutes on ice; FITC-conjugated goat antirat immunoglobulin G (IgG) (1:100) was used for secondary staining of macrophage-labeled cells. All samples were then washed twice with staining buffer and fixed with 1% paraformaldehyde in PBS. The fixed cell samples were stored at 4°C under shade until scanned. FCASscan analysis (Becton-Dickinson, Franklin Lakes, NJ, USA) was performed on 10^4 cells using CellQuest software. Control cells were scanned with isotope-matched rat IgG and FITC-conjugated antibodies.

Histopathology, immunohistochemistry, and immunofluorescence

Four micron sections were cut from paraffin blocks and processed for hematoxylin-eosin staining or indirect immunoperoxidase staining. For the latter, after deparaffinization and rehydration, the sections were treated with proteinase K and boiled by microwave in citrate buffer for unmasking. Next, the sections were immersed in 3% H_2O_2 in methanol in order to inhibit endogenous peroxidase and nonspecific reaction products before flooding with 5% BSA in PBS. Rabbit anti-FSP1 (1:500) [27, 28], rabbit anti-type I collagen (1:400) [36], rat anti-Mac-3 (1:50), and rat anti-platelet-endothelial cell adhesion molecule-1 (PECAM-1) (CD31) (1:50) (PharMingen) were applied as primary antibodies followed by immunoenzyme reaction using biotin-conjugated antirabbit IgG or antrat IgG (1:500) (American Qualex, San Clemente, CA, USA), and a Vectastain ABC Standard Kit (Vector Laboratories, Burlingame, CA, USA). Reaction development was accomplished using diaminobenzidine (DAB) as substrate (for detection of CD31, more intensive digestion and longer microwave exposure were needed). Ten visceral peritoneal fields at 150× magnification were assessed quantitatively in each immunostained section using a color image computer analyzer (Mac SCOPE, version 2.5, Mitani Corp., Hukui, Japan). Immunohistochemical stainings were expressed as % area of reaction product within the subserosal stroma between the mesothelium and intestinal smooth muscle layer, including the mesothelium. Single or dual immunofluorescence was performed on 4 μm cryostat sections. The primary antibodies were employed as follows: goat anti-heat shock protein 47 (HSP47) (1:100) (Santa Cruz Biotechnology, Santa Cruz, CA, USA), anti-MCP-1 (1:100) (Santa Cruz Biotechnology), anti-vascular endothelial growth factor (VEGF) (1:100) (Santa Cruz Biotechnology), rabbit anti-FSP-1 (1:500), anti-tk protein (1:500) (generous gift from W.C. Summers, Yale University) conjugated with FITC using a FITC Protein Labeling Kit (Boehringer Mannheim GmbH, Mannheim, Germany), rat anti-Mac-3 (1:50), or FITC-conjugated rat antimouse CD4 and antimouse CD8 were used; a secondary antibody (Rhodamine-conjugated antigoat IgG and antirabbit IgG (1:500) (Chemicon International, Temecula, CA, USA) or FITC-conjugated anti-rabbit IgG and anti-rat IgG (1:500; American Qualex)) followed where necessary. These sections were analyzed under confocal microscope (MRC600) (Bio-Rad Laboratories, Hercules, CA). All of the secondary antibodies were isolated by immunoaffinity chromatography and absorbed for dual labeling. Control measures included omitting the primary antibody or substituting the primary antibody with species-specific normal IgG.

Detection of apoptotic cells

DNA fragmentation within apoptotic cell nuclei was detected using the MEBSTAIN Apoptosis Kit Direct (Medical and Biological Laboratories, Nagoya, Japan). After deparaffinization and treatment with proteinase K, histologic sections were incubated for 1 hour at 37°C with FITC-deoxyuridine triphosphate (dUTP) and terminal deoxynucleotidyl transferase, the latter linking FITC-dUTP to the 3′-OH fragmented ends of DNA. Immunocytochemistry with anti-FSP1 antibody and Rhodamine-conjugated antirabbit IgG was performed to colocalize apoptosis with FSP1 expression.

Indirect ELISA

Some of the small bowel tissues were sonicated in a cold radioimmunoprecipitation assay (RIPA) lysis buffer [1% nitroprusside-40, 0.1% sodium dodecyl sulfate (SDS), 100 μg/mL phenylmethylsulfonylfluoride, 0.5% sodium deoxycholate, 1 mmol/L sodium orthovanadate, 2 μg/mL aprotinin, 2 μg/mL antipain, and 2 μg/mL leupeptin in PBS), and the homogenates were centrifuged for 5 minutes at 4°C. The protein concentration in the supernatant was determined using a BCA Protein Assay Kit (Pierce, Rockford, IL, USA). Ninty-six-well multititer ELISA plates were coated in triplicate with 5 μg of protein sample/well [36]. The plates were incubated overnight at room temperature. After coating, the plates

were washed three times with 0.15 mol/L NaCl and 0.05% Tween 20 washing solution. After washing, the plates were blocked with 2% BSA and 0.1% Tween 20 in PBS buffer for 30 minutes at 37°C. After blocking, the plates were rewashed with washing solution and then incubated with rabbit anti-type I collagen (1:1000) in incubation buffer for 1 hour at room temperature. Preimmune serum was used as control. The plates were rewashed and incubated with alkali phosphatase-conjugated antirabbit IgG (1:1000) (Sigma Chemical Co., St. Louis, MO, USA) in incubation buffer for 1 hour at room temperature. After washing thoroughly, substrate, disodium p-nitrophenyl phosphate (5 μg/mL) (Sigma Chemical Co.) was added, and the absorbance was measured with an ELISA autoreader (Microplate Reader Model 3550) (Bio-Rad) at 450 nm.

Plasma biochemistry

At the end of the study, plasma samples collected from 3 mice in each group that did not receive PET were analyzed biochemically. The serum albumin levels were determined with the bromcresol green method (A/G B test, Wako, Osaka, Japan). Blood urea nitrogen, creatinine, total cholesterol, alanine aminotransferase, and alkaline phosphatase levels were measured with an autoanalyzer (Dry-Chem 3000, Fuji, Tokyo, Japan).

Modified PET

Modified PET was carried out to determine the ultrafiltration capacity of peritoneum following PFS. Five milliliters of 7% glucose dialysis fluid was instilled into the peritoneal cavity and maintained there for 2 hours. At the end of the PET, each mouse was sacrificed by cervical dislocation under ether anesthetic. Remaining CAPD fluid was drained through the catheter, and then laparotomy was performed to collect residual intraperitoneal fluid and tissue samples. The drainage volume was weighed, and the glucose concentration was determined with Dry-Chem 3000.

Statistical analysis

Values were presented as means ± SE. Statistical differences between groups were evaluated by analysis of variance, followed by Duncan's multiple range test, with $P < 0.05$ used to detect significance.

RESULTS

General observations in mice with PFS

Chronic administration of saline for 4 weeks in control mice (Fig. 1) did not significantly alter the visceral peritoneum (representative section; Fig. 2A). Although chronic administration of CHG saline into the peritoneal cavity was not lethal, most PFS mice did not gain weight during the 4 weeks study period. After 2 weeks of every other day administration of CHG, the visceral peritoneal histology from PFS mice demonstrated a mesothelium largely intact with a thickened subserosa. By week 4, the subserosal peritoneal tissue of PFS mice was significantly thickened with fibrocellular components (representative sections; Fig. 2 B and C); $FSP1^+$ fibroblasts were beginning to accumulate at week 2 (Fig. 2E) and in greater numbers by week 4 (Fig. 2F) compared to the subserosa of control mice (Fig. 2D). Most of the other cells in the subserosa of PFS mice were Mac-3^+ macrophages (Fig. 2G); Mac-3^+ cells were $FSP1^-$ by FACSscan (data not shown). $CD4^+$ and $CD8^+$ T lymphocytes were only identified occasionally in the subserosal peritoneum of PFS mice (data not shown). Furthermore, increased deposition of type I collagen and an increased number of $CD31^+$ vascular endothelial cells in the subserosal peritoneum of PFS mice were found in fibrotic areas (Fig. 2 H and I). The numbers of $FSP1^+$ fibroblasts and Mac-3^+ macrophages, the amount of type I collagen and the extent of vascularity in the subserosal tissue each increased over time ($P \leq 0.05$) (Fig. 3). Although the number of Mac-3^+ macrophages were fewer than the number of $FSP1^+$ fibroblasts throughout the study, the macrophages invaded the subserosal tissue at weeks 1 to 2 before the fibroblasts increased in the number (Fig. 3 A and B). The presence of proliferating fibroblasts and infiltrating macrophages was followed by increasing deposits of type I collagen and neoangiogenesis (Fig. 3 C and D). Dual immunocytochemistry of the subserosal peritoneum of PFS mice revealed that most of the MCP-1, HSP47, or $VEGF^+$ stromal cells were simultaneously positive for FSP1 (Fig. 4 A to C), suggesting that peritoneal fibroblasts play a role in the enrollment of macrophages, collagen production, and neoangiogenesis in PFS. Overall, the peritoneal histology in control mice was nearly normal, and chronic insertion of the catheter itself, at least for 4 weeks, did not cause any substantial changes to the visceral peritoneum. All the controls for immunohistochemistry were without significant background signals.

Deletion of fibroblasts in mice with PFS

In preliminary studies, we evaluated several general parameters prior to undertaking the deletion experiments. First, flow cytometric analysis of splenocytes derived from FSP1.Δtk mice, with or without GCV treatment, revealed no remarkable alterations in the cellular composition of the spleen. For example, the percentage of $CD4^+$ and $CD8^+$ T lymphocytes, and Mac-3^+ macrophages from FSP1.Δtk mice receiving GCV were 27% ± 2%, 14% ± 2%, and 27% ± 3%, respectively, and 23% ± 2%, 11% ± 2%, 24% ± 2%, respectively, in FSP1.Δtk mice not receiving GCV. Second, we observed in peritoneal fibrosis-transgenic mice that fibroblasts in the peritoneum at week 2 were simultaneously positive for Δtk protein and FSP1 (Fig. 4d). Third, a nonlethal dose of

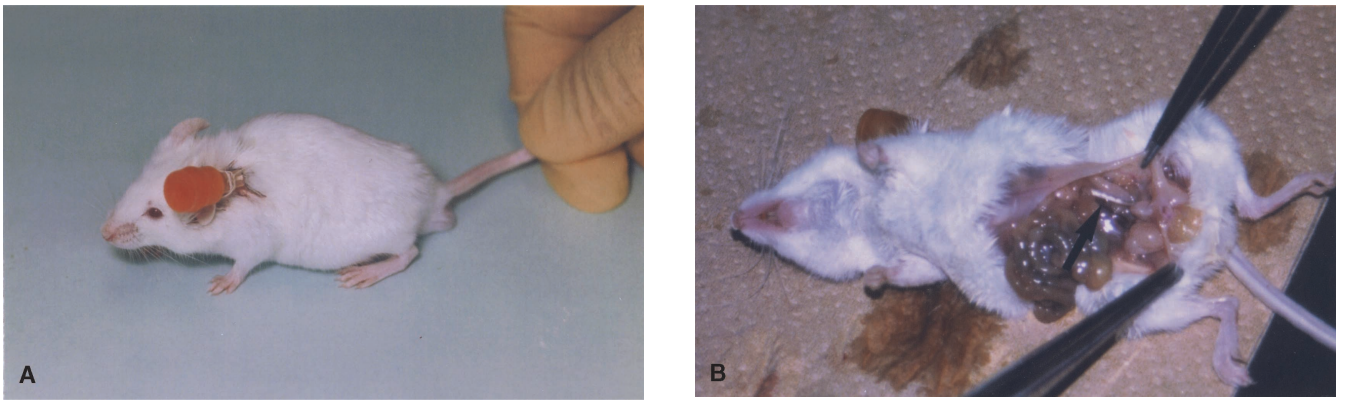

Fig. 1. Murine model of peritoneal fibrosing syndrome (PFS). (*A*) A 21 gauge plastic catheter was inserted from the back into the peritoneal cavity, fixed to the back skin, and maintained for 4 weeks. Each mouse was kept individually in one cage. (*B*) The catheter tip was located intraperitoneally (arrow). After each insertion procedure, normal saline was infused and drained through the catheter to confirm the location of the catheter tip.

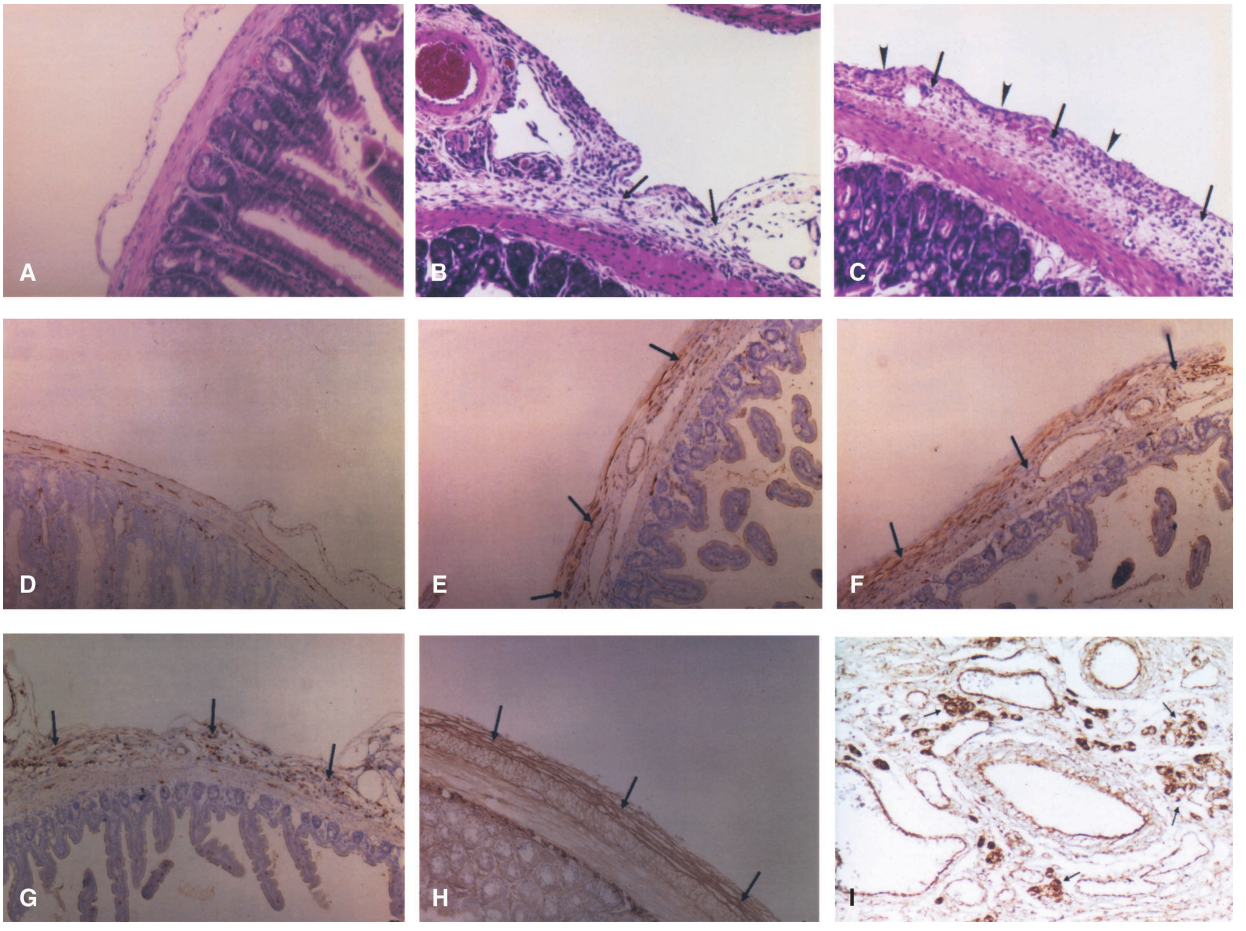

Fig. 2. Typical histopathology of murine peritoneal fibrosing syndrome (PFS). (*A*) Visceral peritoneum of control-wild-type mice at week 4. Subserosal stroma was thin and few cellular components were observed (hematoxylin-easin stain, 150×). (*B*) Visceral peritoneum of peritoneal fibrosis-wild-type mice at week 2. Subserosal stroma was thickened (arrows) and contained cellular components (hematoxylin-eosin stain, 150×). (*C*) Visceral peritoneum of peritoneal fibrosis-wild-type mice at week 4. Subserosal stroma was significantly thickened (arrows) and both cellular and acellular areas were observed. Much of mesothelium remained intact (arrowheads) (hematoxylin-eosin stain, 150×). (*D*) There were few fibroblast-specific protein-1 ($FSP1^+$) fibroblasts in the subserosal stroma of control-wild-type mice at week 4 diaminobenzidine (DAB) (150×). (*E*) There were numerous $FSP1^+$ fibroblasts in the subserosal stroma (arrows) of peritoneal fibrosis-wild-type mice at week 2 (DAB, 150×). (*F*) These $FSP1^+$ fibroblasts in the cellular area of the subserosal stroma (arrows) remained in peritoneal fibrosis-wild-type mice at week 4 (DAB, 150×). (*G*) There were a number of $Mac\text{-}3^+$ macrophages in the subserosal stroma (arrows) of peritoneal fibrosis-wild-type mice at week 2 (DAB, 150×). (*H*) There was significant deposition of type I collagen in the subserosal stroma (arrows) in peritoneal fibrosis-wild-type mice at week 4 (DAB, 150×). (*I*) The thickened subserosal tissue in peritoneal fibrosis-wild-type mice at week 4 was rich in $CD31^+$ small vessels (arrows) (DAB, 200×).

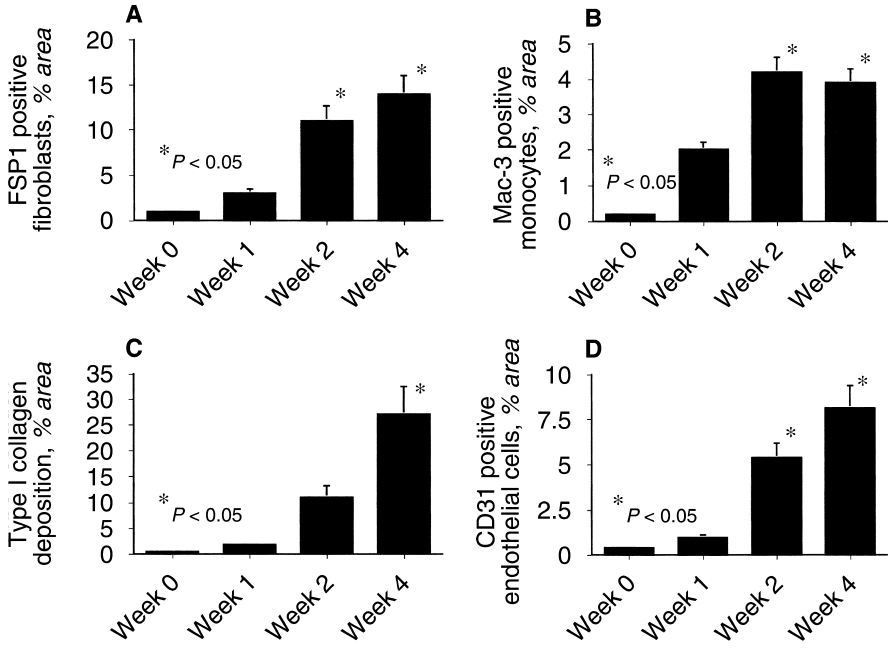

Fig. 3. Quantitative assessment of fibroblast-specific protein-1 (FSP1$^+$) fibroblasts, Mac-3$^+$ macrophages, and extent of type I collagen deposition in peritoneal fibrosis-wild-type mice. (*A*) The number of FSP1$^+$ fibroblasts in the subserosal stroma significantly increased over time. (*B*) The number of Mac-3$^+$ macrophages in the subserosal stroma significantly increased by week 2 and remained until week 4. (*C*) The amount of type I collagen deposition in the subserosal stroma of the peritoneum increased significantly by week 4. (*D*) The hypervascularity in the subserosal stroma was significant at week 4.

GCV (50 mg/kg) once a day by catheter infusion was well tolerated for a treatment protocol of 2 weeks (data not shown). Finally, the metabolic profile of mice from all groups was not significantly different from each other (data not shown).

In experiments to formally test the role of peritoneal fibroblasts in mice with PFS, the visceral peritoneum of peritoneal fibrosis-wild-type + GCV mice after 4 weeks of CHG saline were fibrotic and significantly thickened compared to peritoneal fibrosis-transgenic + GCV mice (Fig. 5 A and B), and seemed substantially similar to peritoneal fibrosis mice in the pilot study. Apoptosis was induced exclusively in FSP1$^+$ fibroblasts (Fig. 4E) in peritoneal fibrosis-transgenic mice with exposure to GCV such that the number of FSP1$^+$ fibroblasts in the peritoneum was significantly reduced below those in peritoneal fibrosis–wild-type mice. The percentage of the apoptotic nuclei was 45.5% $\pm$ 5.5% among 40 $\pm$ 4 FSP1$^+$ fibroblasts observed in a 300$\times$ field of subserosal stroma from peritoneal fibrosis-transgenic mice at week 4, but only 2.0% $\pm$ 0.4% among 49 $\pm$ 5 FSP1$^+$ fibroblasts in peritoneal fibrosis-wild-type mice ($P < 0.05$) (Figs. 5 C and D and 6 A).

When the proliferation of FSP1$^+$ fibroblasts was attenuated in peritoneal fibrosis-transgenic mice receiving GCV, the number of Mac-3$^+$ macrophages and CD31$^+$ endothelial cells, and the accumulation of type I collagen were also reduced in the peritoneum of peritoneal fibrosis-transgenic mice ($P \leq 0.05$) (Figs. 5 E to I and 6 B to D), leaving the subserosal tissues of the visceral peritoneum in peritoneal fibrosis-transgenic mice considerably intact. The peritoneum of control-transgenic mice and control-wild-type mice had no significant abnormalities (data not shown). Quantification analyses by indirect ELISA also demonstrated that deletion of fibroblasts in peritoneal fibrosis-transgenic mice treated with GCV reduced type I collagen deposition to control levels ($P \leq 0.05$) (Fig. 7).

Modified PET

At the conclusion of the 4 week study, each group of mice (peritoneal fibrosis-transgenic, peritoneal fibrosis-wild-type, control-transgenic, and control-wild-type) underwent a modified PET. The drainage volume and glucose concentration of each group were measured (Fig. 8). These indices were significantly lower in peritoneal fibrosis-wild-type + GCV mice compared to those measured in peritoneal fibrosis-transgenic + GCV mice ($P \leq 0.05$), suggesting that selective deletion of fibroblasts in peritoneal fibrosis-transgenic mice reduced glucose absorption and preserved ultrafiltration.

DISCUSSION

We observed that the number of FSP1$^+$ fibroblasts in the subserosal stroma of mice with PFS increased significantly over a 4-week interval following chronic exposure to CHG saline. At week 2, the PFS lesions generated in peritoneal fibrosis-transgenic mice showed increasing numbers of FSP1$^+$ fibroblasts. GCV treatment started at that time for an additional 2 weeks rescued the peritoneum from PFS by decreasing the number of fibroblasts to the control levels via apoptosis. Our approach to peritoneal rescue was associated with a decrease in monocyte infiltration, collagen deposition, and neoangiogenesis.

Since studies of fibroblasts in vivo have been limited

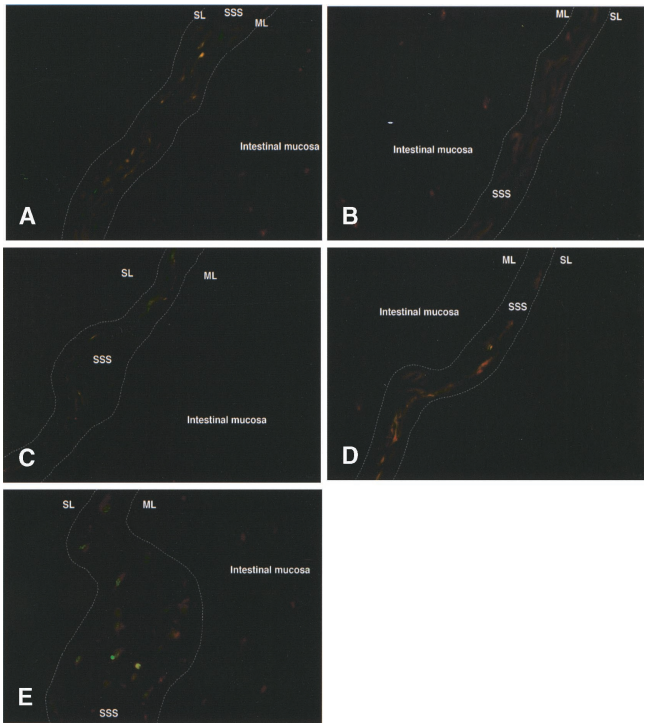

Fig. 4. Characterization of peritoneal fibroblast-specific protein-1 (FSP1$^+$) fibroblasts in the subserosal stroma. (*A*) Immunofluorescence of FSP1 (in red) and monocyte chemoattractant protein-1 (MCP-1) (in green) in peritoneal fibrosis-wild-type mice at week 4. There were some stromal cells in yellow in the subserosal stroma, indicating that some fibroblasts produced MCP-1 (merged image, 150×). (*B*) Using two labels, FSP1 (in red) and heat shock protein 47 (HSP47) (in green), there were some stromal cells in yellow in the subserosal stroma of peritoneal fibrosis-wild-type mice at week 4, indicating that FSP1$^+$ fibroblasts contributed to collagen production (merged image, 150×). (*C*) Immunofluorescence of FSP1 (in red) and vascular endothelial growth factor (VEGF) (in green) in peritoneal fibrosis-transgenic mice at week 2. Some of FSP1$^+$ fibroblasts in the subserosal stroma (in yellow) were simultaneously positive for VEGF, suggesting their contribution to neoangiogenesis (merged image, 150×). (*D*) Immunofluorescence of FSP1 (in red) and thymidine kinase (tk) protein (in green) in peritoneal fibrosis-transgenic mice at week 2. FSP1$^+$ fibroblasts in the subserosal stroma were simultaneously positive for tk protein, yielding yellow color (merged image, 150×). (*E*) Many of the FSP1$^+$ fibroblasts were selectively killed by gancyclovir (GCV) treatment via apoptosis (arrows) on colocalization of FSP1 expression (in red) and apoptotic nuclei (in green) in peritoneal fibrosis-transgenic mice at week 4 following GCV treatment (merged image, 300×). Abbreviations are: SL, serosal layer; SSS, subserosal stroma; ML, muscular layer.

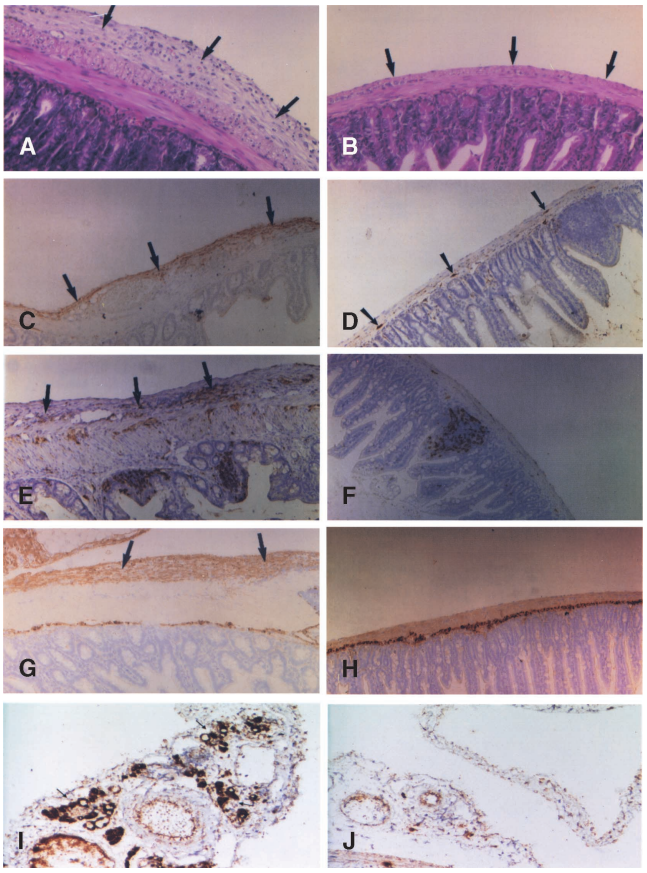

Fig. 5. Typical histopathology of peritoneal fibroblast-specific protein (PFS) in peritoneal fibrosis-transgenic and peritoneal fibrosis-wild-type mice treated with gancyclovir (GCV). (*A*) The subserosal stroma of the visceral peritoneum (arrows) in peritoneal fibrosis-wild-type mice was thickened and fibrous (hematoxylin-eosin stain, 150×). (*B*) With GCV treatment, the subserosal stroma of the visceral peritoneum (arrows) in peritoneal fibrosis-transgenic mice remained thin and contained few cellular components (hematoxylin-eosin stain, 150×). (*C*) There were a number of fibroblast-specific protein-1 (FSP1$^+$) fibroblasts in the subserosal stroma (arrows) from peritoneal fibrosis-wild-type mice diaminobenzidine (DAB) (150×). (*D*) GCV treatment reduced the number of FSP1$^+$ fibroblasts in the subserosal stroma (arrows) of peritoneal fibrosis-transgenic mice (DAB, 150×). (*E*) There were a number of Mac-3$^+$ macrophages in the subserosal stroma (arrows) of peritoneal fibrosis-wild-type mice (DAB, 150×). (*F*) GCV treatment reduced the number of Mac-3$^+$ macrophages in the subserosal stroma of peritoneal fibrosis-transgenic mice (DAB, 150×). (*G*) There was a significant deposition of type I collagen in the subserosal stroma (arrows) of peritoneal fibrosis-wild-type mice (DAB, 150×). (*H*) There was no significant deposition of type I collagen in the subserosal stroma of peritoneal fibrosis-transgenic mice (DAB, 150×). (*I*) Increased vascularity by CD31 staining was evident in the subserosal tissue of peritoneal fibrosis-wild-type mice (arrows) (DAB, 200×). (*J*) There was no significant vascularity in the subserosal tissue of peritoneal fibrosis-transgenic mice (DAB, 200×).

by a lack of fibroblasts-specific markers, we took advantage of the marker, FSP1 [27, 29]. FSP1 belongs to the S-100 superfamily and is associated with the regulation of cell shape and motility [27, 36]. Using anti-FSP1 antibody, we have previously demonstrated that the number of FSP1$^+$ fibroblasts increase in parallel with the progression of renal fibrosis [27, 28, 31]. The same was true in the present study. Our FSP1.Δtk transgenic mouse on exposure to GCV had some additional advantages, one of which is that GCV administration induces apoptosis only in proliferating fibroblasts [31]. This approach works in connective tissues (peritoneum) as well as in complex organs [26, 31].

In the early days of CAPD in humans, it was believed that regular exposure of peritoneal membranes to antiseptics might reduce the risk of peritonitis [14]. However,

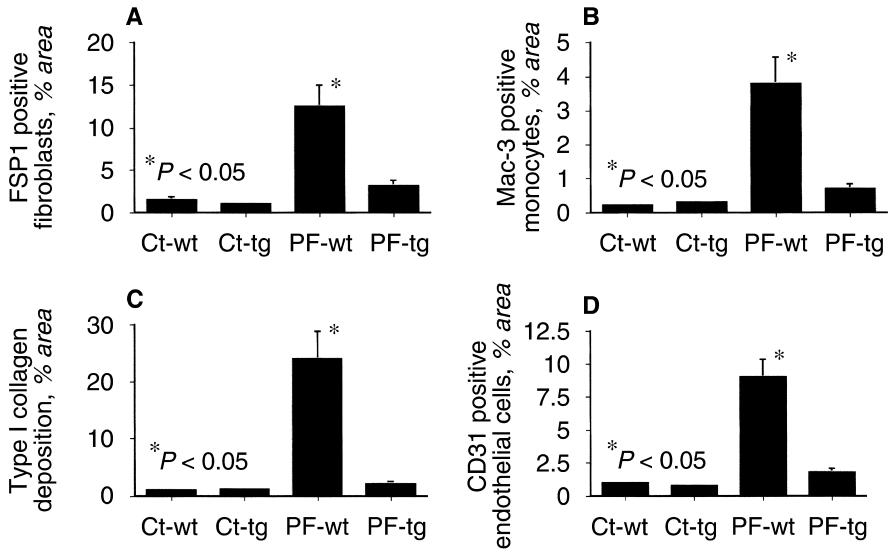

Fig. 6. Quantitative assessment of peritoneal fibroblast-specific protein (PFS) histopathology in peritoneal fibrosis-transgenic (PF-tg) and peritoneal fibrosis-wild-type (PF-wt) mice treated with gancyclovir (GCV). (*A*) The number of fibroblast-specific protein-1 (FSP1$^+$) fibroblasts in peritoneal fibrosis-transgenic mice was significantly reduced to the control levels (Ct-wt and Ct-tg) by GCV treatment. (*B*) The number of Mac-3$^+$ macrophages in peritoneal fibrosis-transgenic mice was reduced to control levels with GCV. (*C*) The amount of type I collagen deposited in the peritoneum of peritoneal fibrosis-transgenic mice was also maintained at control levels by deletion of fibroblasts. (*D*) Neoangiogenesis was also inhibited in the subserosal tissue of peritoneal fibrosis-transgenic mice.

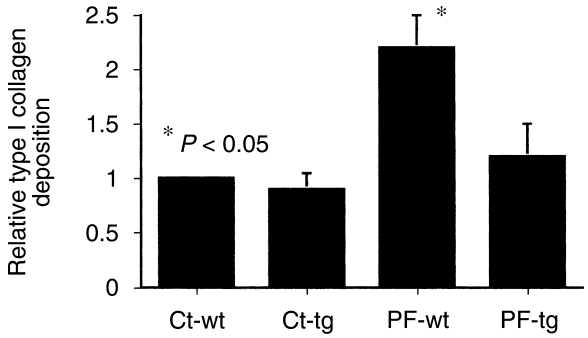

Fig. 7. Quantitative analysis of type I collagen in the peritoneal subserosa by indirect enzyme-linked immunosorbent assay (ELISA). The amount of type I collagen deposited in small bowel subserosa of peritoneal fibrosis-wild-type (PF-wt)mice treated with gancyclovir (GCV) was significantly greater than in peritoneal fibrosis-transgenic mice (PF-tg). Collagen in these peritoneal fibrosis-transgenic mice was significantly reduced to control levels (Ct-wt and Ct-tg) by deletion of fibroblasts following GCV treatment.

exposure to chlorhexidine in alcohol was identified early as responsible for an outbreak of sclerosing peritonitis [30]. This observation was confirmed by toxicologic experiments in animals [17, 19, 30, 37]. Accordingly, we introduced chlorhexidine into the peritoneum of mice to generate PFS [19, 30, 38]. Constant exposure of the mesothelium to chlorhexidine is thought to disrupt mesothelial tight junctions followed by crystalline damage to the subserosal stroma [14, 30]. Persistent serositis results from prolonged exposure to this or other toxic metabolites and creates an inflammatory response that predisposes to PFS.

Recent studies in CAPD patients suggest that peritoneal fibroblasts may derive from mesothelium by epithelial-mesenchymal transition [13]. Based on in vitro observations, peritoneal fibroblasts both respond to proinflammatory stimuli with proliferation and increased synthesis of matrix, and contribute to the cytokine network secreting immunologically active molecules into the peritoneum [39]. We demonstrated by immunofluorescence that FSP1$^+$ fibroblasts in the peritoneum express MCP-1, a macrophages chemoattractant [40], and HSP47, a collagen chaperone [41]. The deletion of fibroblasts significantly reduced the number of infiltrating macrophages and the accumulation of type I collagen in the peritoneum, suggesting that fibroblasts are involved in the enrollment of circulating macrophages and the production of type I collagen. At an early phase of PFS, macrophages are attracted by activated resident cells in the peritoneum, including mesothelial cells, fibroblasts, and infiltrated macrophages themselves [42–44]. Furthermore, fibroblasts likely anchor infiltrating macrophages, and fibroblast deletion subsequently erased the macrophages that would have otherwise infiltrated the subserosal tissue (Figs. 2G and 5F). These infiltrating macrophages can accelerate fibrogenesis by releasing profibrogenic cytokines and the fibroblasts growth factors described above [29, 45]. The reduction in their numbers might indirectly attenuate PFS. Our findings suggest that macrophages and fibroblasts cofacilitate each other, leading to a vicious cycle perpetuating fibrogenesis, and that deletion of FSP1$^+$ fibroblasts can interrupt this cycle. The degree of experimental fibrosis may depend on the strain variability of mice. Compared to other strains, Balb/c mice (like we used in this study) may not form extensive fibrotic tissue under some experimental conditions [46–48]. We nevertheless observed significant peritoneal fibrosis in Balb/c mice.

We also observed enhanced glucose absorption and loss of ultrafiltration capacity in peritoneal fibrosis-wild-type mice treated with GCV. This functional deteriora-

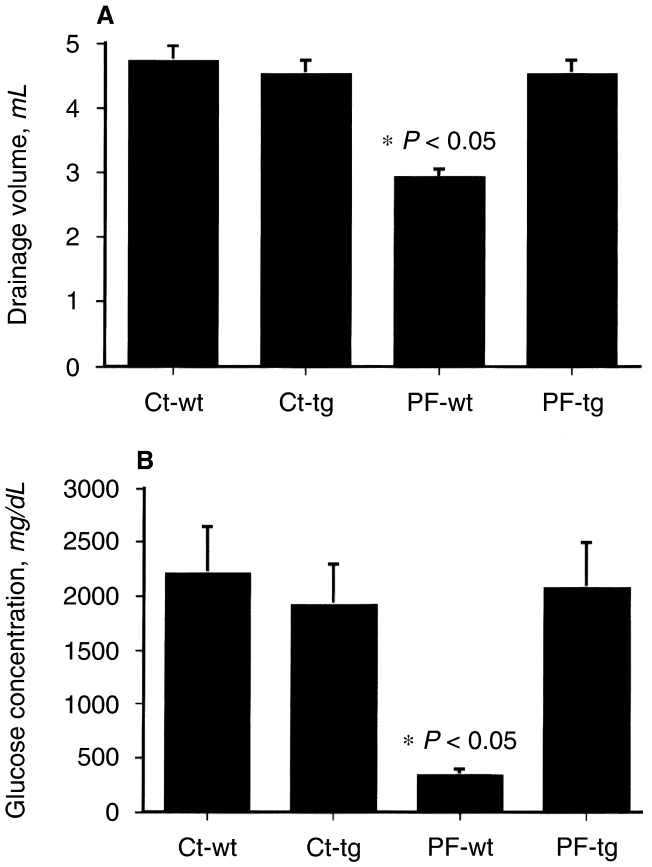

Fig. 8. Modified peritoneal equilibrium test (PET). (*A*) The volume of fluid drained from peritoneal fibrosing syndrome (PFS) mice. The volume of fluid drained from peritoneal fibrosis-wild-type (PF-wt) mice was significantly less than that of peritoneal fibrosis-transgenic mice (PF-tg) treated with gancyclovir (GCV) ($P \leq 0.05$), and similar to the control levels (Ct-wt and Ct-tg) in mice not treated with chlorhexidine gluconate (CHG) saline. This suggests that ultrafiltration capacity was preserved in peritoneal fibrosis-transgenic mice by deletion of fibroblasts compared to peritoneal fibrosis-wild-type mice. (*B*) The glucose concentration of drained fluid in peritoneal fibrosis-wild-type mice was significantly lower ($P \leq 0.05$) than that of peritoneal fibrosis-transgenic mice treated with GCV, and similar to the control levels in mice not treated with CHG saline. This suggests that the ultrafiltration failure observed in peritoneal fibrosis-wild-type mice was due to the increased diffusion of glucose through the peritoneal membrane.

tion of the peritoneum is similar to the same well-known complication of long-term CAPD. Several different mechanisms for loss of filtration across the peritoneum have been described [1, 49–51]. Some authors emphasize the role of increased solute transport to explain the loss of ultrafiltration due to peritoneal hypervascularity [52, 53], whereas others suggest the possible impact of changing lymphatic or peritoneal fluid absorption into peritoneal tissue [54, 55]. A third possibility is that the formation of adhesions and sclerosis results in a hyperpermeable peritoneum even with loss of surface area [1]. Finally, impaired efficiency of the osmotic agent in peritoneal dialysate, without change in solute transport, may contribute to loss of ultrafiltration, perhaps related to alterations in transcellular water channels (aquaporin-1) in the vascular endothelium [56–58]. Among these mechanisms, enhanced glucose absorption due to hypervascularity in the peritoneal membrane is the most common explanation for loss of ultrafiltration in CAPD [51–53].

In the present study, we also observed that fibroblasts express VEGF, an angiogenic growth factor, which might be involved in neoangiogenesis of subserosal tissue [53, 59]. Several investigators reported that fibroblasts producing VEGF provide a basic framework for proliferating endothelial cells that form vascular structures [60–62]. Therefore, antifibrotic therapy by deleting $FSP1^+$ fibroblasts may be important in the prevention of $CD31^+$ neoangiogenesis in subserosal tissue. We suggest that controlling the number of $FSP1^+$ fibroblasts assists in maintaining mesothelial architecture, while reducing the infiltration of macrophages, collagen accumulation, and neoangiogenesis that preserves peritoneal function.

Although CAPD patients are not given chlorhexidine any more, there are a growing number of patients on CAPD suffering from PFS and ultrafiltration failure [1–5, 12, 14]. The histopathologic findings in our model of PFS are similar to the peritoneal characteristics of CAPD patients after a couple of episodes of peritonitis [12, 14, 63] and supports the clinical relevance of our experimental system. A few experimental trials to prevent PFS using pirfenidone or glycosaminoglycans have been reported [11, 19]. To our knowledge, it is the first study demonstrating that peritoneal fibroblasts play a pivotal role in the process of PFS. Their conditional deletion has therapeutic potential.

ACKNOWLEDGMENTS

The authors thank S. Yamada, J. Takahashi, and M. Otobe for their technical assistance. H.O. was supported by an Extramural Research Grant from Baxter Healthcare Corporation. E.G.N. was supported in part by grants DK-46282 and DK-55926 from the National Institutes of Health. A portion of this work was presented at the 33rd Annual Meeting of the American Society of Nephrology in Toronto, Canada, 2000.

Reprint requests to Hirokazu Okada, M.D., Ph.D., Assistant Professor of Medicine, Department of Nephrology, Saitama Medical College, 38 Morohongo, Moroyama-Machi, Irumagun, Saitama 350-04 Japan. E-mail: hirookda@saitama-med.ac.ip

REFERENCES

1. Heimbuerger O, Wang T, Lindholm B: Alterations in water and solute transport with time on peritoneal dialysis. *Perit Dial Int* 19:S83–S90, 1999
2. Schreiber MJ: Membrane viability in the long-term peritoneal dialysis patient. *Perit Dial Int* 17:S19–S24, 1996
3. Struijk D, Krediet R, Koomen G, *et al*: A prospective study of peritoneal transport in CAPD patients. *Kidney Int* 45:1739–1744, 1994
4. Davies S, Bryan J, Phillips L, *et al*: Longitudinal changes in peritoneal kinetics: The effects of peritoneal dialysis and peritonitis. *Nephrol Dial Transplant* 11:498–506, 1996
5. Miyata T, Devuyst O, Kurokawa K, *et al*: Toward better dialysis

compatibility: Advances in the biochemistry and pathophysiology of the peritoneal membranes. *Kidney Int* 61:375–386, 2002
6. Rubin J, Herrera G, Collins D: An autopsy study of the peritoneal cavity from patients on continuous ambulatory peritoneal dialysis. *Am J Kidney Dis* 18:97–102, 1991
7. Suassuna J, Das Neves F, Hartley R, *et al*: Immunohistochemical studies of the peritoneal membrane and infiltrating cells in normal subjects and in patients on CAPD. *Kidney Int* 46:443–454, 1994
8. Honda K, Nitta K, Horita S, *et al*: Morphological changes in the peritoneal vasculature of patients on CAPD with ultrafiltration failure. *Nephron* 72:171–176, 1996
9. Honda K, Nitta K, Horita S, *et al*: Accumulation of advanced glycation end products in the peritoneal vasculature of continuous ambulatory peritoneal dialysis patients with low ultra-filtration. *Nephrol Dial Transplant* 14:1541–1549, 1999
10. Mateijsen M, van der Wal A, Hendriks P, *et al*: Vascular and interstitial changes in the peritoneum of CAPD patients with peritoneal sclerosis. *Perit Dial Int* 19:517–525, 1999
11. Fracasso A, Baggio B, Ossi E, *et al*: Glycosaminoglycans prevent the functional and norphological peritoneal derangement in an experimental model of peritoneal fibrosis. *Am J Kidney Dis* 33:105–110, 1999
12. Coles G, Topley N: Long-term peritoneal membrane changes. *Adv Renal Replace Ther* 7:289–301, 2000
13. Yanez-Mo M, Lara-Pezzi E, Selgas R, *et al*: Peritoneal dialysis and epithelial-to-mesenchymal transition of mesothelial cells. *N Engl J Med* 348:403–413, 2003
14. Dobbie J: Pathogenesis of peritoneal fibrosing syndromes (sclerosing paeritonitis) in peritoneal dialysis. *Perit Dial Int* 12:14–27, 1992
15. Nagy J: Peritoneal membrane morphology and function. *Kidney Int* 50:S2–S11, 1996
16. Di Paolo N, Sacchi G, De Mia M, *et al*: Morphology of the peritoneal membrane during continuous ambulatory peritoneal dialysis. *Nephron* 44:204–211, 1986
17. Mackow R, Argy W, Winchester J, *et al*: Sclerosing encapsulating peritonitis in rats induced by long-term intraperitoneal administration of antiseptics. *J Lab Clin Med* 112:363–371, 1988
18. Slater N, Cope G, Raftery A: Mesothelial hyperplasia in response to peritoneal dialysis fluid: A morphometric study in the rat. *Nephron* 58:466–471, 1991
19. Suga H, Teraoka S, Ota K, *et al*: Preventive effect of pirfenidone against experimental sclerosing peritonitis in rats. *Exp Toxic Pathol* 47:287–291, 1995
20. Park M, Heimbuerger O, Bergstroem J, *et al*: Evaluation of an experimental rat model for peritoneal dialysis: Fluid and solute transport characteristics. *Nephrol Dial Transplant* 9:404–412, 1994
21. Suzuki K, Khanna R, Nolph K, *et al*: Expected white blood cell counts and differentials in a rat model of peritoneal dialysis. *Perit Dial Int* 15:142–146, 1995
22. Gotloib L, Shostak A, Wajsbrot V, *et al*: The cytochemical profile of vasceral mesothelium under the influence of lactated-hyperosmolar peritoneal dialysis solutions. *Nephrol* 69:466–471, 1995
23. Nakamoto M: Pathognesis of peritoneal fibrosis and peritoneal small vessel changes. *Perit Dial Int* 16:S39–S41, 1996
24. Levine S, Saltzman A: Abdominal cocoon: An animal model for a complication of peritoneal dialysis. *Perit Dial Int* 16:613–616, 1996
25. Nakamoto H, Imai H, Ishida Y, *et al*: New animal models for encapsulating peritoneal sclerosis-role of acidic solution. *Perit Dial Int* 21(Suppl 3):S349–S353, 2001
26. Okada H, Danoff T, Fischer A, *et al*: Identification of a novel cis-acting element for fibroblast-specific transcription of the FSP1 gene. *Am J Physiol* 275:F306–F314, 1998
27. Strutz F, Okada H, Lo CW, *et al*: Identification and characterization of a fibroblast marker: FSP1. *J Cell Biol* 130:393–405, 1995
28. Okada H, Ban S, Nagao S, *et al*: Progressive renal fibrosis in murine polycystic kidney disease: An immunohistochemical observation. *Kidney Int* 58:587–597, 2000
29. Okada H, Strutz F, Danoff T, *et al*: Possible mechanisms of renal fibrosis. *Contrib Nephrol* 118:147–154, 1996
30. Junor B, Briggs J, Forwell M, *et al*: Sclerosing peritonitis—the contribution of chlorhexidine in alcohol. *Perit Dial Bull* 5:101–104, 1985
31. Iwano M, Fischer A, Okada H, *et al*: Conditional abatement of tissue fibrosis using nucleoside analogs to selectively corrupt DNA replication in transgenic fibroblasts. *Mol Ther* 3:149–159, 2001
32. Eddy A: Molecular basis of renal fibrosis. *Pediatr Nephrol* 15:290–301, 2000
33. Goldstein CS, Bomalaski JS, Zurier RB, *et al*: Analysis of peritoneal macrophages in continuous ambulatory peritoneal dialysis patients. *Kidney Int* 26:733–740, 1984
34. Okada H, Moriwaki K, Kalluri R, *et al*: Inhibition of monocyte chemoattractant protein-1 expression in tubular epithelium attenuates tubulointerstitial alteration in rat Goodpasture syndrome. *Kidney Int* 57:927–936, 2000
35. Neilson EG, McCafferty E, Feldman A, *et al*: Spontaneous interstitial nephritis in kdkd mice. I. An experimental model of autoimmune renal disease. *J Immunol* 133:2560–2565, 1984
36. Okada H, Danoff T, Kalluri R, *et al*: Early role of Fsp1 in epithelial-mesenchymal transformation. *Am J Physiol* 273:F563–F574, 1997
37. Mackow R, Winchester J, Argy W, *et al*: Sclerosing encapsulating peritonitis in rats: An experimental study with intraperitoneal antiseptics. *Contrib Nephrol* 57:213–218, 1987
38. Lo W, Chan K, Leung A, *et al*: Sclerosing peritonitis complicating prolonged use of chlorhexidine in alcohol in the connection procedure for continuous ambulatory peritoneal dialysis. *Perit Dial Int* 11:166–172, 1992
39. Joerres A, Ludat K, Sander K, *et al*: The peritoneal fibroblast and the control of peritoneal inflammation. *Kidney Int* 50:S22–S27, 1996
40. Gu L, Rutledge B, Fiorillo J, *et al*: In vivo properties of monocyte chemoattractant protein-1. *J Leukoc Biol* 62:577–580, 1997
41. Nagata K: Expression and function of heat shock protein 47: A collagen-specific molecular chaperone in the endoplasmic reticulum. *Matrix Biol* 16:379–386, 1998
42. Lee SK, Kim BS, Yang WS, *et al*: High glucose induces MCP-1 expression partly via tyrosine kinase-AP-1 pathway in peritoneal mesothelial cells. *Kidney Int* 60:55–64, 2001
43. Beavis MJ, Williams JD, Hoppe J, *et al*: Human peritoneal fibroblast proliferation in 3-dimensional culture: Modulation by cytokines, growth factors and peritoneal dialysis effluent. *Kidney Int* 51:205–215, 1997
44. Rapoport J, Hausmann MJ, Chaimovitz C: The peritoneal immune system and continuous ambulatory peritoneal dialysis. *Nephron* 81:375–380, 1999
45. Nathan C: Secretory products of macrophages. *J Clin Invest* 79:319–326, 1987
46. Barth R, Hanchett LA, Baecher-Allan CM: Mapping susceptibility genes for the induction of pulmonary fibrosis in mice. *Chest* 121(Suppl):21S, 2002
47. Chiaramonte MG, Cheever AW, Malley JD, *et al*: Studies of murine schistosomiasis reveal interleukin-13 blockade as a treatment for established and progressive liver fibrosis. *Hepatology* 34:273–282, 2001
48. Kolb M, Bonniaud P, Galt T, *et al*: Differences in the fibrogenic response after transfer of active transforming growth factor-b1 gene to lungs of "fibrosis-prone" and "fibrosis-resistant" mouse strains. *Am J Respir Cell Mol Biol* 27:141–150, 2002
49. Ho-Dac-Pannekeet M, Atasever B, Struijk D, *et al*: Analysis of ultrafiltration failure in peritoneal dialysis patients by means of standard peritoneal permeability analysis. *Perit Dial Int* 17:144–150, 1997
50. Korbet S: Evaluation of ultrafiltration failure. *Adv Renal Replace Ther* 5:194–204, 1998
51. Agrawal A, Nolph KD: Management of high peritoneal transporters. *Perit Dial Int* 20(Suppl 2):S160–S165, 2000
52. Heimbeurger O, Waniewski J, Werynski A, *et al*: Peritoneal transport in CAPD patients with permanent loss of ultrafiltration capacity. *Kidney Int* 38:495–506, 1990
53. Krediet RT, Zweers MM, van der Wal AC, *et al*: Neoangiogenesis in the peritoneal membrane. *Perit Dial Int* 20(Suppl 2):S19–S25, 2000
54. Heimbuerger O, Waniewski J, Werynski A, *et al*: Lymphatic absorption in CAPD patients with loss of ultrafiltration capacity. *Blood Purif* 13:327–339, 1995

55. Mactier R, Khanna R, Twardowski Z, *et al*: Ultrafiltration failure in continuous ambulatory peritoneal dialysis due to excessive peritoneal cavity lymphatic absorption. *Am J Kidney Dis* 10:461–466, 1987
56. Ho-Dac-Pannekeet M, Mulder J, Weening J, *et al*: Demonstration of aquaporin-CHIP in peritoneal tissue of uremic and CAPD patients. *Perit Dial Int* 16:S54–S57, 1996
57. Monquil M, Imholz A, Struijk D, *et al*: Does impaired transcellular water transport contribute to net ultrafiltration failure during CAPD? *Perit Dial Int* 15:42–48, 1995
58. Yang B, Folkesson H, Yang J, *et al*: Reduced osmotic water permeability of the peritoneal barrier in aquaporin-1 knockout mice. *Am J Physiol* 276:C76–C81, 1999
59. Zweers M, de Waart D, Struijk D, *et al*: The growth factors VEGF and TGF-β1 in peritoneal dialysis. *J Lab Clin Med* 134:124–132, 1999
60. Velazquez OC, Snydedr R, Liu AJ, *et al*: Fibroblast-dependent differentiation of human microvascular endothelial cells into capillary-like 3-dimensional networks. *FASEB J* 16:1316–1318, 2002
61. Trompezinski S, Denis A, Vinche A, *et al*: IL-4 and interferon-g differentially modulate vascular endothelial growth factor release from normal human keratinocytes and fibroblasts. *Exp Dermatol* 11:224–231, 2002
62. Cho ML, Cho CS, Min SY, *et al*: Cyclosporine inhibition of vascular endothelial growth factor production in rheumatoid synovial fibroblasts. *Arthritis Rheum* 46:1202–1209, 2002
63. Park M: Factors increasing severity of peritonitis in long-term peritoneal dialysis patients. *Adv Renal Replace Ther* 5:185–193, 1998